



High Frequency Square Wave Voltage Injection Based Inductance Identification for PMSM Sensorless Control

Yang Ge^(✉), Weizhang Song, and Yang

School of Electrical Engineering, Xian University of Technology, Xian 710048, China
gy@xaut.edu.cn

Abstract. The sensorless control performance of permanent magnet synchronous motor (PMSM) is greatly degraded by inductance mismatch in the medium and high speed region. Therefore, an on-line inductance identification method based on high-frequency (HF) square wave voltage injection, which can be embedded in PMSM sensorless control, is proposed. By injecting the high-frequency square wave voltage in dq -axis, the HF current response is obtained, and the envelope of HF current is extracted. On this basis, an inductance identification algorithm is designed. The estimated inductance values are used to update the values in flux observer. This method is applicable to both surface mounted and interior rotor structures. The simulation results indicate that the proposed method can accurately identify the inductance value and improve the sensorless performance.

Keywords: Permanent magnet synchronous motor (PMSM) · Sensorless control · Inductance identification · High-frequency square wave injection

1 Introduction

The PMSM sensorless control has attracted extensive attention because it can effectively reduce costs, improve space utilization and reliability [1]. In the medium and high speed region, the sensorless control mainly adopts the model estimation method [2–5], i.e., using the voltage-flux model to estimate the back-EMF or rotor flux, and then calculate the rotor position and speed.

The model estimation method relies on the accurate resistance and inductance values. However, in practice, it is hard to obtain them directly. Moreover, their values could change under complex working conditions. For example, the resistance will change with the operating temperature, and the inductance value could change with the current under the magnetic circuit saturation [6, 7]. At medium and high speed, the influence of inductance error will be more obvious than that of resistance error. Therefore, the on-line inductance identification is very necessary to improve the sensorless control performance.

At present, some research on parameters identification of PMSM under sensorless control have been carried out. In [8], an inductance identification method, in which the current differential and DC voltage measurement is required, is proposed. This method

achieves inductance identification by measuring current differential in each PMW cycle in real time. However, it requires high-performance hardware and high bandwidth current sensors. In [9, 10], it is proposed to obtain a new voltage equation by injecting rotating high-frequency voltage and extracting the amplitude of high-frequency current for inductance identification. This method requires to inject dq -axis voltage at the same time. But, at higher speed, the identification accuracy will be degraded due to the increased coupling effect. Besides, the frequency of the rotating voltage is difficult to be high enough, so the influence on the motor speed of injected voltage will be larger, and the resistance voltage will also lead to identification error. In [11, 12], a parameter identification method based on DC signal injection is proposed. But this method has to work until all current injections are finished, so the real-time property is not satisfactory. In addition, this method needs to assume that the inductance value remains constant under different DC currents, but due to the magnetic circuit saturation, this assumption is difficult to meet in practice.

In order to achieve the online identification of inductance for PMSM sensorless control. An online inductance identification scheme based on high-frequency (HF) square wave voltage injection is presented. By injecting HF square wave voltage on d -axis and q -axis by turns, the HF current response is obtained and the coupling effect is reduced. Then, using the triangular characteristics of current response, its envelope can be extracted on this basis, the identification algorithm of dq -axis inductance is designed. Since the frequency of square wave voltage can be 0.5 times of the switching frequency, this method has little effect on the motor speed. The simulation results indicates that the proposed method can accurately identify the inductance value and improve the sensorless performance.

2 Problem Formulation

2.1 The Model-Based Sensorless Control of PMSM

Assuming the winding of PMSM is symmetric and the saturation effect is neglected, the $\alpha\beta$ -axis voltage-flux model is given by

$$\begin{cases} u_\alpha = p\psi_{r\alpha} + R_s i_\alpha + L_q(p i_\alpha) \\ u_\beta = p\psi_{r\beta} + R_s i_\beta + L_q(p i_\beta) \end{cases} \tag{1}$$

where $i_{\alpha,\beta}$ and $u_{\alpha,\beta}$ denote the $\alpha\beta$ -axis currents and voltages; $\psi_{r\alpha} = [\psi_r + (L_d - L_q)i_d] \cos \theta$ and $\psi_{r\beta} = [\psi_r + (L_d - L_q)i_d] \sin \theta$ denote the “equivalent flux”; R_s , L_d and L_q denote stator resistance and dq -axis inductance. Based on Eq. (1), $\psi_{r\alpha}$ and $\psi_{r\beta}$ can be estimated by second-order generalized integrator (SOGI), which is presented as

$$\frac{dv}{dt} = [(u_\alpha - \hat{R}_s i_\alpha - v)k - \hat{\omega} \int_0^t v dt] \hat{\omega} \tag{2}$$

According to [13], v will track $u_\alpha - R_s i_\alpha$, and $\int_0^t v dt$ can be simultaneously obtained. Then, $\psi_{r\alpha}$ can be estimated by $\hat{\psi}_{r\alpha} = \int_0^t v dt - \hat{L}_q i_\alpha$, where the hat “^” indicates the estimated value hereafter. Similarly, $\hat{\psi}_{r\beta}$ can be also estimated using SOGI. Then, both the position and speed will be acquired by PLL. We can see in above process, the accurate resistance and inductance are necessary for position and speed estimation.

2.2 The Influence of Parameter Error on Position Estimation

Assuming $\hat{R}_s \neq R_s$ and $\hat{L}_q \neq L_q$, the following equation can be obtained from Eq. (1)

$$\begin{cases} \hat{\psi}_{r\alpha} = \psi_{r\alpha} - \tilde{R}_s \int_0^t i_\alpha dt - \tilde{L}_q i_\alpha \\ \hat{\psi}_{r\beta} = \psi_{r\beta} - \tilde{R}_s \int_0^t i_\beta dt - \tilde{L}_q i_\beta \end{cases} \quad (3)$$

where $\tilde{R}_s = \hat{R}_s - R_s$ and $\tilde{L}_q = \hat{L}_q - L_q$. Then, multiply $\begin{pmatrix} \cos \hat{\theta} & \sin \hat{\theta} \\ -\sin \hat{\theta} & \cos \hat{\theta} \end{pmatrix}$ on both sides of Eq. (3), it yields

$$\begin{cases} \psi_{rm} = [\psi_r + (L_d - L_q)i_d] \cos \tilde{\theta} - (\tilde{R}_s / \omega)i_q - \tilde{L}_q i_d \\ 0 = [\psi_r + (L_d - L_q)i_d] \sin \tilde{\theta} + (\tilde{R}_s / \omega)i_d - \tilde{L}_q i_q \end{cases} \quad (4)$$

Then, the position error can be deduced as

$$\tilde{\theta} = \arcsin[(\tilde{R}_s i_d) / (\psi_m \omega) - (\tilde{L}_q i_q) / \psi_m] \quad (5)$$

where $\psi_m = \psi_r + (L_d - L_q)i_d$. We can see the position error resulted by \tilde{R}_s relates to i_d and ω , and the position error resulted by \tilde{L}_q is determined by i_q . For surface-mounted PMSM, i_d is generally controlled as zero, and i_q produces the electromagnetic torque, so the effect of \tilde{L}_q will be more severe than that of \tilde{R}_s . For interior PMSM, both \tilde{R}_s and \tilde{L}_q will lead to the position error, especially under heavy load.

3 The HF Square Voltage Injection Based Inductance Identification

3.1 The HF Voltage Equation

From above section, we can see that the inductance error will lead to the larger position error in medium and high speed region. So, in this paper, an inductance identification method is proposed. Injecting the HF square voltage, and ignoring the resistance voltage and back-EMF, we have

$$\begin{cases} u_{din} = L_d p i_{din} - \omega L_q i_{qin} \\ u_{qin} = L_q p i_{qin} + \omega L_d i_{din} \end{cases} \quad (6)$$

where u_{din} , u_{qin} , i_{din} and i_{qin} are HF voltages and currents. It should be noted that, unlike the traditional high-frequency signal injection method which is generally used at low-speed, the coupling term should not be ignored at higher speed. Since the frequency of the square voltage can be very high, the influence on the rotor speed will be slight. And considering the high-frequency voltage drop of the resistance is very small, we can ignore the back-EMF and the resistance voltage.

3.2 The Inductance Identification Algorithm

In this section, the inductance identification algorithm is presented.

First, at high-speed region, the effect of coupling term $\omega L_q i_{qin}$ and $\omega L_d i_{din}$ is larger. To reduce the coupling effect, the d -axis and q -axis square voltages are injected by turns, i.e., when u_{din} is injected, $u_{qin} = 0$; and when u_{qin} is injected, $u_{din} = 0$. Here, we take injecting u_{din} as an example. Since $u_{qin} = 0$, i_{qin} can be ignored, then we have

$$u_{din} = L_d p i_{din} \tag{7}$$

Since u_{din} is a square wave, i_{din} will be a triangular wave. Therefore, if we extract the envelope of i_{din} , i.e., peak value of the triangular wave. L_d can be calculated using Eq. (7).

Let $i_d = i_{df} + i_{din}$, where i_{df} denotes fundamental wave in i_d . Assuming i_{df} is constant in $T_i/2$, where T_i is the injection cycle time, and considering the characteristic of triangular wave, we have

$$\begin{cases} i_d(k_1) - i_d(k_0) = 2I_{dh} \text{sgn}(u_{qh}(k_0)) \\ i_d(k_1) + i_d(k_0) = 2i_{df}(k_0) \end{cases} \tag{8}$$

where I_{dh} is the envelope of i_{qh} , i.e., peak value of the triangular wave. Using Eq. (8), both I_{dh} and i_{df} can be extracted. Considering I_{qh} is a constant or slowly varying variable, we can use the low pass filter to reduce the noise of current with little information loss.

Then, according to Eq. (7), we have

$$|u_{dh}| = L_d \frac{4I_{dhL}}{T_i} \tag{9}$$

where I_{dhL} is the filtered I_{dh} . Define

$$H = (|u_{din}| - \frac{\hat{L}_d}{4} T I_{dinL})^2 \tag{10}$$

It can be known that the optimum value of L_d can make H become minimum. Using gradient theory, the identification algorithm is designed as

$$\frac{d\hat{L}_d}{dt} = \lambda (|u_{din}| - \frac{\hat{L}_d}{4} T I_{dinL}) - \frac{1}{4} T I_{dinL} \tag{11}$$

where $\lambda > 0$ is the adaptive parameter which determines the convergence rate.

When q -axis voltage is injected, the identification algorithm of q -axis inductance can be designed similarly. In order to improve the real-time performance, the dq -axis voltage injection period of should be shorter. In this paper, it set as 0.1 s.

Figure 1 shows the block diagram of inductance identification algorithm. When u_{din} is injected, u_{qin} is zero, L_d is identified using i_{din} , and at the same time, L_q is also identified using the data obtained in last period. Since this method does not rely on the rotor saliency, it is applicable to surface mounted and interior PMSM. Figure 2 shows the overall system including the sensorless control of PMSM.

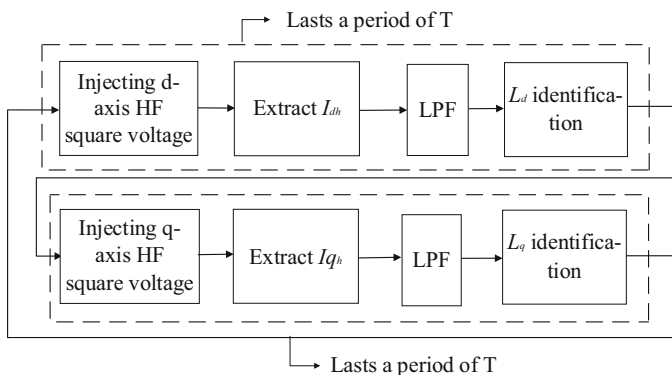


Fig. 1. The diagram of inductance identification

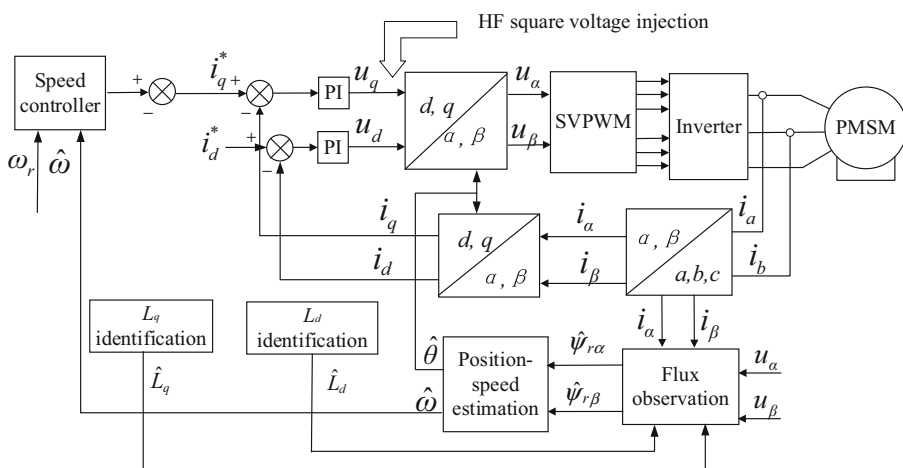


Fig. 2. The diagram of the overall system

Table 1. Parameters of PMSM

| Parameters | Value |
|----------------------------|--|
| Stator resistance R_s | 2Ω |
| d -axis inductance L_d | 10 mH |
| q -axis inductance L_q | 5 mH |
| Rotor flux ψ_r | 0.2 Wb |
| Pole pairs n_p | 4 |
| Moment of inertia J | $5 \times 10^{-4} \text{ kg}\cdot\text{m}^2$ |

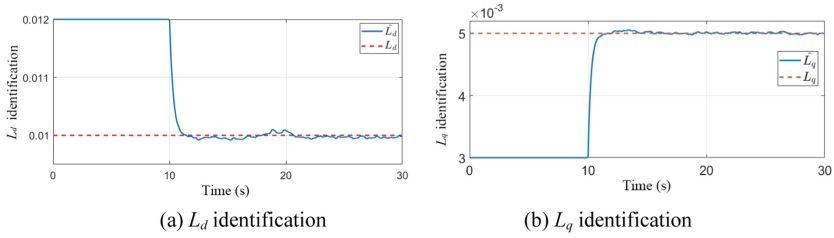


Fig. 3. Inductance identification results

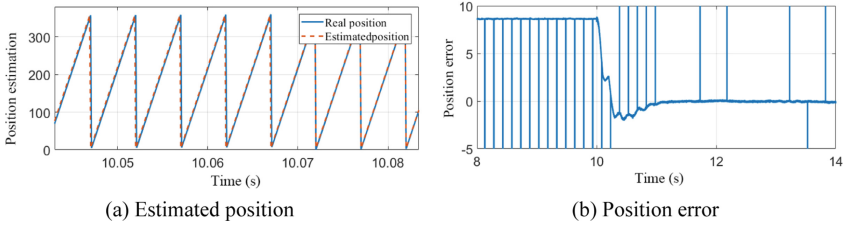


Fig. 4. Rotor position estimation and its error

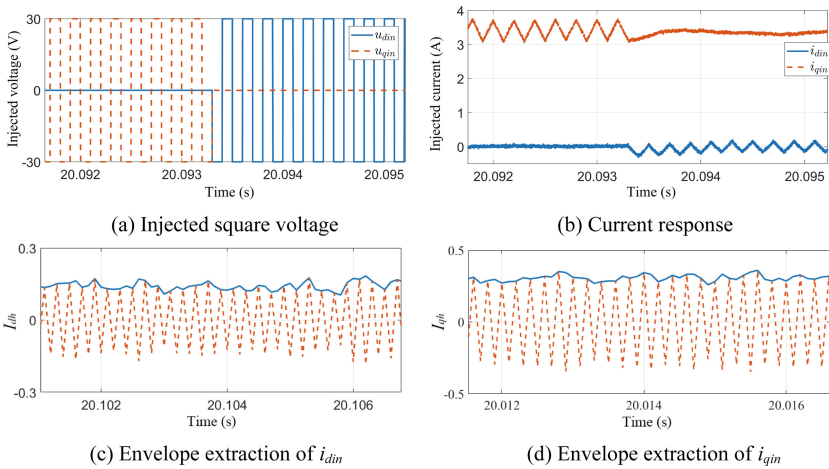


Fig. 5. Injected voltage and the current response

4 Simulation Results

The simulation is carried out in this section. The motor parameters used in simulation are shown in Table 1.

Figure 3 shows the inductance estimation results. We can see that after the identification algorithm is enabled, the estimated inductance can quickly converge from the initial value to the actual value. Figure 4 shows the position estimation and its error. When the inductance error exists, the position error is also large. As the estimated inductance

converges to its actual value, the position estimation error also converges to around zero. Figure 5 shows the injected voltage, the current response and its envelope extraction. It can be seen that the envelope of the current response can be accurately acquired using Eq. (8). We can also see the extracted envelope contains high-frequency noise, which can be reduced by low-pass filter, and it will not affect the inductance identification accuracy.

5 Conclusion

In order to resolve the inductance mismatch problem in sensorless PMSM control, an online inductance identification method based on high-frequency (HF) square wave voltage injection is proposed. By injecting HF square wave voltage on dq -axis by turns, the HF current response is obtained. And the envelope of current response can be extracted using the characteristic of triangular wave. Based on that, an identification algorithm of inductance is designed. The simulation results validate the effectiveness of this method.

References

1. Ding, L., Li, Y., Zargari, N.R.: Discrete-time SMO sensorless control of current source converter-fed PMSM drives with low switching frequency. *IEEE Trans. Ind. Electron.* **68**(3), 2120–2129 (2021)
2. Repecho, V., Bin Waqar, J., Biel, D.: Zero speed sensorless scheme for permanent magnet synchronous machine under decoupled sliding-mode control. *IEEE Trans. Ind. Electron.* **69**(2), 1288–1297 (2021)
3. Devanshu, A., Singh, M., Kumar, N.: An improved nonlinear flux observer based sensorless FOC IM drive with adaptive predictive current control. *IEEE Trans. Power Electron.* **35**(1), 652–666 (2020)
4. Zhang, C.J., Wang, H.Z., Liu, W.F.: Rotor position and speed estimation of permanent magnet synchronous motor based on wide-band synchronous fundamental frequency extraction filter. *Trans. China Electrotech. Soc.* **37**(4), 882–891 (2022)
5. Ge, Y., Yang, L.H., Ma, X.K.: Sensorless control of PMSM using generalized extended state observer and adaptive resistance estimation. *IET Electric Power Appl.* **14**(1), 2062–2073 (2020)
6. Mingardi, D., Morandin, M., Bolognani, S., Bianchi, N.: On the proprieties of the differential cross-saturation inductance in synchronous machines. *IEEE Ind. Appl.* **53**(2), 991–1000 (2017)
7. Chen, Y., Zhu, Z., Howe, D.: Calculation of d - and q -axis inductances of PM brushless ac machines accounting for skew. *IEEE Trans. Magn.* **41**(10), 3940–3942 (2005)
8. Bui, M.X., Rahman, M.F., Guan, D.Q.: A new and fast method for on-line estimation of d and q axes inductances of interior permanent magnet synchronous machines using measurements of current derivatives and inverter DC-bus voltage. *IEEE Trans. Ind. Electron.* **66**(10), 7488–7497 (2019)
9. Wu, C., Zhao, Y., Sun, M.: Multi parameter online identification of permanent magnet synchronous motor using measured voltage. *Trans. China Electrotech. Soc.* **40**(13), 4329–4339 (2020)
10. Li, F., Che, J., Liu, D.: Dynamic inductance identification method and rotor position estimation error compensation strategy for IPMSM. *Trans. China Electrotech. Soc.* **33**(23), 5418–5426 (2018)

11. Feng, G., Lai, C., Mukherjee, K., et al.: Current injection-based online parameter and VSI nonlinearity estimation for PMSM drives using current and voltage DC components. *IEEE Trans. Transp. Electrif* **2**(2), 119–128 (2016)
12. Shi, T., Liu, H., Chen, W.: Parameter identification of surface mounted permanent magnet synchronous motor considering nonlinear factors of inverter. *Trans. China Electrotech. Soc.* **32**(7), 77–83 (2017)
13. Xu, W., Jiang, Y., Mu, C., Blaabjerg, F.: Improved nonlinear flux observer-based second-order SOIFO for PMSM sensorless control. *IEEE Trans. Power Electron* **34**(1), 565–579 (2018)